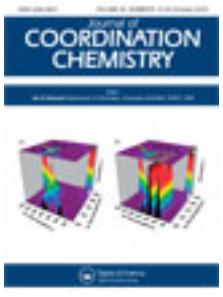


Journal of Coordination Chemistry
Publication details, including instructions for authors and subscription information:
http://www.tandfonline.com/loi/gcoo20

# Synthesis and structure of a macrocyclic dinuclear Zn(II) complex together with DNA-binding and kinetic studies

Yun-Feng Chen [a], Ming Liu [a], Jia-Wei Mao [a b], Hui-Ting Song [a], Hong Zhou [a] & Zhi-Quan Pan [a]

[a] Key Laboratory for Green Chemical Process of Ministry of Education, Wuhan Institute of Technology, Wuhan 430073, P.R. China

[b] College of Chemistry and Molecular Sciences, Wuhan University, Wuhan 430072, P.R. China

Accepted author version posted online: 01 Aug 2012.Published online: 14 Aug 2012.

To cite this article: Yun-Feng Chen, Ming Liu, Jia-Wei Mao, Hui-Ting Song, Hong Zhou & Zhi-Quan Pan (2012) Synthesis and structure of a macrocyclic dinuclear Zn(II) complex together with DNA-binding and kinetic studies, Journal of Coordination Chemistry, 65:19, 3413-3423, DOI: 10.1080/00958972.2012.717690

To link to this article: http://dx.doi.org/10.1080/00958972.2012.717690

*Journal of Coordination Chemistry*
Vol. 65, No. 19, 10 October 2012, 3413–3423



# Synthesis and structure of a macrocyclic dinuclear Zn(II) complex together with DNA-binding and kinetic studies

YUN-FENG CHEN†, MING LIU†, JIA-WEI MAO†‡, HUI-TING SONG†, HONG ZHOU† and ZHI-QUAN PAN*†

†Key Laboratory for Green Chemical Process of Ministry of Education, Wuhan Institute of Technology, Wuhan 430073, P.R. China
‡College of Chemistry and Molecular Sciences, Wuhan University, Wuhan 430072, P.R. China

(*Received 19 January 2012; in final form 2 July 2012*)

A new macrocyclic dinuclear Zn(II) complex, $[Zn_2(OAc)L]\cdot ClO_4$ ($H_2L$ was obtained by condensation between 3,3′-(ethane-1,2-diylbis(benzylazanediyl))bis(methylene)bis(2-hydroxy-5-methylbenzaldehyde) and aniline (1 : 2 molar ratio)), was synthesized and characterized by spectroscopy, elemental analysis, and single-crystal X-ray diffraction. The interactions of the complex with DNA have been measured by UV spectroscopy and viscosity experiment. The interaction of the complex with calf thymus DNA has a binding constant of $1.18 \times 10^4\,mol^{-1}\,L$. Phosphate hydrolysis of the complex was investigated using bis(4-nitrophenyl)phosphate as the substrate. The observed first-order rate constant is $4.23 \times 10^{-5}\,s^{-1}$.

*Keywords*: Dinuclear Zn(II) complex; Crystal structure; DNA-binding constant; Catalytic activities



## 1. Introduction

Polynuclear metal complexes have received considerable interest for their special topologies and interesting properties, such as optical [1], electronic [2], magnetic [3, 4], catalytic [5, 6], and biological [7–9]. Condensation between substituted 2,6-diformyl phenols and diamines in the presence of metal ions construct macrocyclic polynuclear metal complexes [10–17]. During the formation of macrocycle, the diamine serves as a bridge to link two aldehyde groups, so the reactions were conducted with a 1 : 1 molar ratio of bridging dialdehydes and diamines. Generally, aliphatic diamines drive the formation of the ring and keep the flexibility of the corresponding macrocycles in contrast with aromatic diamines. Flexibility of the macrocycles is key to catalytic activities [18, 19]. To investigate the relationship between structures and properties of polynuclear metal complexes, we want to obtain polynuclear metal complexes with diverse structures. In this article, we report the synthesis and crystal structures of a new macrocyclic dinuclear Zn(II) complex by condensation between diamine-bridged

*Corresponding author. Email: zhiqpan@163.com; tracy180@126.com


ISSN 0095-8972 print/ISSN 1029-0389 online 
http://dx.doi.org/10.1080/00958972.2012.717690

dialdehyde and aniline with 1 : 2 molar ratio. Although monoamine was used in this template-directed synthesis, the obtained complex still adopted dinuclear macrocyclic configuration instead of mononuclear or polymeric forms. The complex exhibits efficient DNA-binding. This complex containing rigid phenyl diimines has good catalytic activity toward phosphate hydrolysis. The reason must be that this complex has intrinsic flexibility, because the ligand is an open-chain structure although there are rigid phenyl imines.



## 2. Experimental

### 2.1. *General procedures*

All chemicals were purchased from commercial sources and used as received. Solvents were dried according to standard procedures and distilled prior to use. Elemental analyses for C, H, and N were performed on a Perkin-Elmer 240 analyzer. IR spectra were taken on a Bruker Vector 22 Spectrophotometer with KBr pellets from 400 to 4000 $cm^{-1}$. ESI-MS spectra were measured on a Varian MAT 311 A instrument. The crystal structure was determined at room temperature using a Bruker SMART CCD based diffractometer.

### 2.2. *Crystal structure determination*

Diffraction intensity data were collected on a SMART CCD area-detector diffractometer at 298 K using graphite monochromated Mo-K$\alpha$ radiation ($\lambda = 0.71073$ Å). Data reduction and cell refinement were performed by SMART and SAINT programs [20]. The structure was solved by direct methods (Bruker SHELXTL) and refined on $F^2$ by full-matrix least squares (Bruker SHELXTL) using all unique data [21]. The non-H atoms in the structure were treated as anisotropic. Hydrogen atoms were located geometrically and refined in a riding mode. Crystallographic parameters and agreement factor are given in table 1.

### 2.3. *Synthesis of the complex*

The dialdehyde **A** 3,3′-(ethane-1,2-diylbis(benzylazanediyl))bis(methylene)bis-(2hydroxy-5-methylbenzaldehyde) was synthesized according to a procedure reported previously [17].

The synthetic pathway to the complex is shown in scheme 1. A methanol solution (10 mL) of $(CH_3COO)_2Zn \cdot 2H_2O$ (0.0439 g, 0.20 mmol) was added dropwise to **A** (0.1072 g, 0.20 mmol) in methanol (15 mL) at room temperature (298 K). A solution of aniline (0.0373 g, 0.40 mmol) in methanol was then added dropwise. The mixture was stirred for 6 h and then $Zn(ClO_4)_2$ (0.0529 g, 0.20 mmol) in methanol (10 mL) was slowly added. The mixture was stirred for 6 h and filtered, and the filtrate was kept undisturbed for a few days. Orange-yellow crystals were filtered off, washed with cold water and methanol, and dried *in vacuo*. Yield: 0.087 g (45%). Anal. Calcd for $C_{48}H_{47}O_8N_4Zn_2Cl$: C, 59.18; H, 4.86; N, 5.75. Found: C, 59.68; H, 4.93; N, 5.64.

Table 1. Crystal data and details of the structure determination for the complex.

| | |
|---|---|
| Empirical formula | $C_{48}H_{47}ClN_4O_8Zn_2$ |
| Formula weight | 974.09 |
| Temperature (K) | 173(2) |
| Wavelength (Å) | 0.71073 |
| Crystal system | Monoclinic |
| Space group | $P2_1/n$ |
| Unit cell dimensions (Å, °) | |
| $a$ | 10.7020(9) |
| $b$ | 17.3772(15) |
| $c$ | 26.660(2) |
| $\alpha$ | 90 |
| $\beta$ | 99.319(2) |
| $\Gamma$ | 90 |
| Volume (Å$^3$), $Z$ | 4892.6(7), 4 |
| Calculated density (Mg m$^{-3}$) | 1.322 |
| Absorption coefficient (Mo-K$\alpha$) (mm$^{-1}$) | 1.089 |
| $F$(000) | 2016 |
| Crystal size (mm$^3$) | $0.16 \times 0.15 \times 0.10$ |
| Reflections collected | 9099 |
| Independent reflections | 9099 [$R$(int) = 0.0000] |
| Absorption correction | Multi-scan |
| Parameters | 573 |
| Goodness of fit on $F^2$ | 0.975 |
| Final $R$ indices [$I > 2\sigma(I)$] | $R_1 = 0.0556$, $wR_2 = 0.1120$ |
| Largest difference peak and hole (e Å$^{-3}$) | 0.746 and −0.538 |

$W = 1/[S^2(F_o^2) + (0.0461P)^2]$ $P = (F_o^2 + 2F_c^2)/3$.

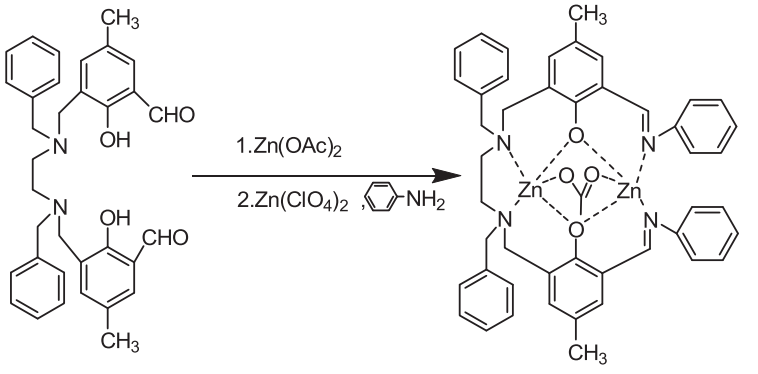


Scheme 1. Synthesis of $[Zn_2(OAc)L]ClO_4$; $ClO_4^-$ is omitted for clarity.

IR spectrum (KBr, cm$^{-1}$): 3061, 2923, 1619(s), 1568(s), 1456, 1308, 1266, 1094(s), 794, 623. The ES-MS spectrum of the Zn(II) complex in methanol solution is dominated by a peak at $m/z$ 875.83, corresponding to $[Zn_2(OAc)L]^+$ ($C_{48}H_{47}O_4N_6Zn_2$, Calcd 875.72).

### 2.4. *DNA-binding experiments*

Calf thymus DNA (CT-DNA) (20 mg) was dissolved in 100 mL of Tris-HCl buffer (50 mmol L$^{-1}$ Tris-HCl, 50 mmol L$^{-1}$ NaCl, pH = 7.4) and kept at 4°C for less than

four days. $A_{260}$ and $A_{280}$ of the above solution were determined on a UV-Vis spectrophotometer and $A_{260}/A_{280}$ should be between 1.8 and 2.0. The DNA concentration was determined *via* absorption spectroscopy using the molar absorption coefficient of $6600\,mol^{-1}\,cm^{-1}$ (260 nm) for CT-DNA [22].

The complex was dissolved in DMF (30%) and Tris-HCl buffer at $0.9 \times 10^{-4}\,mol\,L^{-1}$. The UV absorption titrations were performed by keeping a concentration of the complex while varying the DNA concentration; a correction was made by subtracting from a blank spectrum with an equivalent amount of DMF. Complex-DNA solutions incubated for 30 min before measurements were made. The intrinsic binding constant $K_b$ was calculated according to the literature [23].

Viscosity measurements of CT-DNA were carried out using a capillary viscometer at $23 \pm 0.1°C$. Flow times were measured with a digital stopwatch and each sample was measured three times and an average flow time was calculated. Data are presented as $(F/F_0)^{1/3}$ *versus* molar ratio of complex to DNA [24], where $F$ is the viscosity of DNA in the presence of complex and $F_0$ is the viscosity of DNA in the absence of complex.

### 2.5. *Cleavage of bis(4-nitrophenyl)phosphate*

Bis(4-nitrophenyl)phosphate (BNPP) is usually used as a DNA model in the investigation of phosphodiesterase activity. The cleavage of BNPP produces 4-nitrophenolate (NP) and 4-nitrophenyl phosphate (NPP). The kinetic measurement was performed by monitoring the UV-Vis absorbance change at 406 nm (assigned to NP) as a function of time at 25°C [25]. Hydrolysis of BNPP by the complex was studied in DMF/Tris-HCl buffer (1/3, v/v) solution at pH = 7.4. The concentrations of BNPP and the complex were $2 \times 10^{-3}\,mol\,L^{-1}$ and $2 \times 10^{-4}\,mol\,L^{-1}$, respectively. Stock solutions were freshly prepared before performing the kinetic measurement and the ionic strength was maintained at $I = 0.10\,mol\,L^{-1}$ with potassium chloride.

## 3. Results and discussion

### 3.1. *Description of the crystal structure*

The title complex is crystallized as $[Zn_2(OAc)L]ClO_4$; the complex structure is shown in figure 1. Crystallographic data and details about the data collection are presented in table 1, and selected bond lengths and angles relevant to the Zn coordination spheres of the complex are listed in table 2. Single-crystal X-ray diffraction analysis shows that the complex crystallizes in the monoclinic space group $P2_1/n$. Each $Zn^{2+}$ is five-coordinate. The remaining sites of the distorted square-pyramidal Zn are coordinated by μ-OAc. The two Zn ions reside in $N_2O_2$ sites of the macrocycle, with Zn–Zn distance of 2.971 Å and with Zn–O–Zn angles of 92.75(10)° and 92.36(10)°. $Zn^{2+}$ are bridged by two phenolates and one acetate. Deviation of the Zn(1) and Zn(2) atoms from the mean plane, formed by O1, O2, N1, and N4 and by O1, O2, N2, and N3, are 0.064 Å and 0.130 Å, respectively. The dihedral angle between the planes is 22.22°. The two benzyl groups are on the same side of the plane. However, the two benzene rings of the anilines were located in a nearly vertical position of the plane. The N1 and N4 distance is 3.305 Å. The centroid distance and the dihedral angle between the phenyl groups of

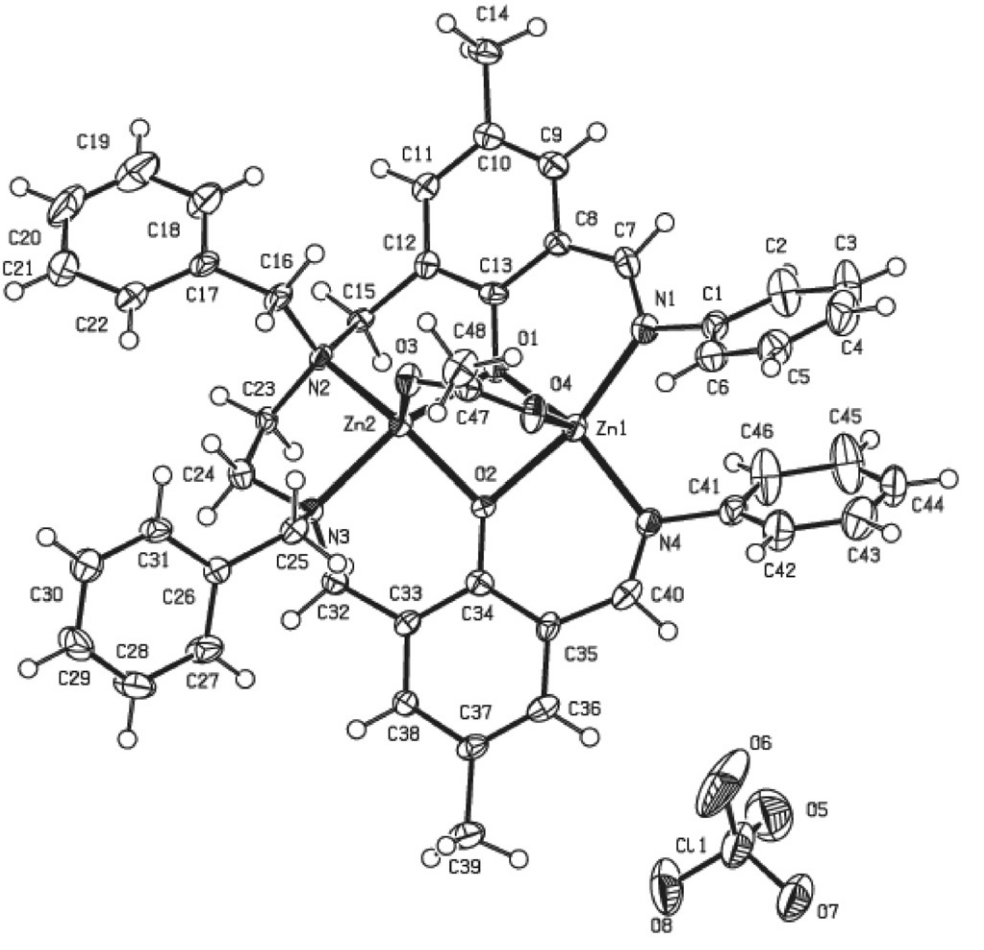


Figure 1. Molecular structure of the complex, showing the atom-numbering scheme. Displacement ellipsoids were drawn at the 30% probability level.

aniline are 3.627 Å and 12.72°, which show that there is $\pi\cdots\pi$ interaction between the two benzene rings of the anilines. The crystal packing is stabilized by hydrogen bond and C–H$\cdots\pi$ interactions. The inversion-related C(15)–H(15B)$\cdots$O(1), C(15)–H(15B)$\cdots$O(2) hydrogen-bond interactions, and C(32)–H(32B)$\cdots\pi$ to C8–C13 rings [H32B$\cdots$ring centroid distance = 2.656 Å] link two macrocycles to form a dimeric structure (figure 2). At the same time, C(14)–H(14A)$\cdots$O(3) and $ClO_4^-$ mediated C(39)–H(39A)$\cdots$O(8) hydrogen-bond interactions forming a 2-D network (figure 3). There are also intramolecular hydrogen-bond interactions at C(6)–H(6)$\cdots$O(4) and C(25)–H(25A)$\cdots$O(4) (hydrogen-bond distances and angles are given in table 2).

### 3.2. *DNA-binding activity*

Absorption spectra of the complex in the absence and presence of CT-DNA at different concentrations (0–60 μmol $L^{-1}$) are shown in figure 4. The spectrum of the complex

Table 2. Selected bond lengths, bond angles, and hydrogen-bonding contacts for the complex.

| | | | |
|---|---|---|---|
| Bond lengths (Å) | | | |
| Zn(1)–O(1) | 2.037(2) | Zn(2)–O(1) | 2.080(2) |
| Zn(1)–O(2) | 2.100(2) | Zn(2)–O(2) | 2.003(2) |
| Zn(1)–O(4) | 2.030(3) | Zn(2)–O(3) | 1.974(3) |
| Zn(1)–N(1) | 2.072(3) | Zn(2)–N(2) | 2.099(3) |
| Zn(1)–N(4) | 2.050(3) | Zn(2)–N(3) | 2.133(3) |
| Zn(1)···Zn(2) | 2.970(7) | | |
| Bond angles (°) | | | |
| O(4)–Zn(1)–O(1) | 104.11(10) | O(4)–Zn(1)–N(4) | 111.77(12) |
| O(1)–Zn(1)–N(4) | 138.83(11) | O(4)–Zn(1)–N(1) | 95.04(12) |
| O(1)–Zn(1)–N(1) | 89.33(11) | N(4)–Zn(1)–N(1) | 106.48(13) |
| O(4)–Zn(1)–O(2) | 91.11(11) | O(1)–Zn(1)–O(2) | 72.94(10) |
| N(4)–Zn(1)–O(2) | 86.57(11) | N(1)–Zn(1)–O(2) | 162.19(11) |
| O(4)–Zn(1)–Zn(2) | 74.36(8) | O(1)–Zn(1)–Zn(2) | 44.39(7) |
| N(4)–Zn(1)–Zn(2) | 128.83(9) | N(1)–Zn(1)–Zn(2) | 123.97(9) |
| O(2)–Zn(1)–Zn(2) | 42.34(6) | O(3)–Zn(2)–O(2) | 108.18(11) |
| O(3)–Zn(2)–O(1) | 100.45(10) | O(2)–Zn(2)–O(1) | 74.06(10) |
| O(3)–Zn(2)–N(2) | 109.65(11) | O(2)–Zn(2)–N(2) | 141.32(11) |
| O(1)–Zn(2)–N(2) | 91.40(11) | O(3)–Zn(2)–N(3) | 103.43(11) |
| O(2)–Zn(2)–N(3) | 91.35(11) | O(1)–Zn(2)–N(3) | 154.98(11) |
| N(2)–Zn(2)–N(3) | 87.57(12) | O(3)–Zn(2)–Zn(1) | 82.19(8) |
| O(2)–Zn(2)–Zn(1) | 44.92(7) | O(1)–Zn(2)–Zn(1) | 43.25(7) |
| N(2)–Zn(2)–Zn(1) | 134.57(9) | N(3)–Zn(2)–Zn(1) | 133.62(8) |

Hydrogen-bonding contacts

| D–H | *d*(D–H) | *d*(H···A) | ∠(D–HA) | *d*(D–HA) | A |
|---|---|---|---|---|---|
| C(15)–H(15B) | 0.99 | 2.60 | 156.6 | 3.529(4) | O(1)$^{\#1}$ |
| C(14)–H(14A) | 0.98 | 2.50 | 163.1 | 3.454(5) | O(3)$^{\#2}$ |
| C(6)–H(6) | 0.95 | 2.37 | 145.3 | 3.205(5) | O(4) |
| C(25)–H(25A) | 0.99 | 2.59 | 120.9 | 3.213(5) | O(3) |
| C(39)–H(39A) | 0.98 | 2.57 | 164.1 | 3.520(5) | O(8) |

Symmetry code: #1: $1-x$, $2-y$, $-z$; #2: $2-x$, $2-y$, $-z$.



shows a very strong absorption at 366 nm, attributed to a metal-to-ligand charge transfer [26, 27]. The band shows a red-shift of about 9 nm and hypochromism of 11.3% after adding DNA. The value of $K_b$ was obtained from the ratio of slope to intercept from the plot of $[(DNA)/(\varepsilon_a - \varepsilon_f)]$ *versus* [DNA] (figure 5). The $K_b$ value is $1.18 \times 10^4\,mol^{-1}\,L$. Comparing the intrinsic binding constant of this Zn(II) complex with those of DNA-intercalative macrocyclic Cu(II) complexes [28], we can deduce that the Zn(II) complex binds to DNA by moderate intercalation. The $K_b$ value is the same as that of reported macrocyclic dinuclear Zn(II) complex (bis-TACN macrocycle bridged by bis-4-methylphenol as ligand, $K_b$ value was $1.16 \times 10^4\,mol^{-1}\,L$) [29]. Structurally, the ligand of the complex may have aromatic conjugation with the stacking base pairs of the DNA helix [11, 30]. We conclude that the open-chain structure of the complex has little effect on DNA-binding.

To further confirm the interaction mode of the complex with DNA, a viscosity study was carried out (figure 6). The specific viscosity of DNA increases with increased concentration of the complex. This again suggests that the binding mode between the complex and DNA may be intercalation [31, 32].

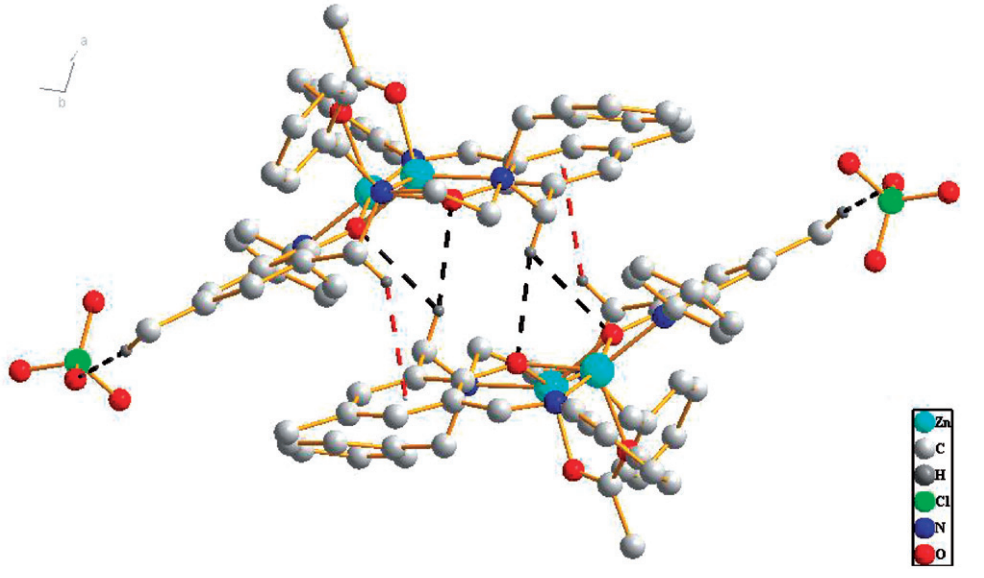


Figure 2. The dimeric structure driven by inversion-related C–H···$\pi$ and C–H···O hydrogen-bond interactions.

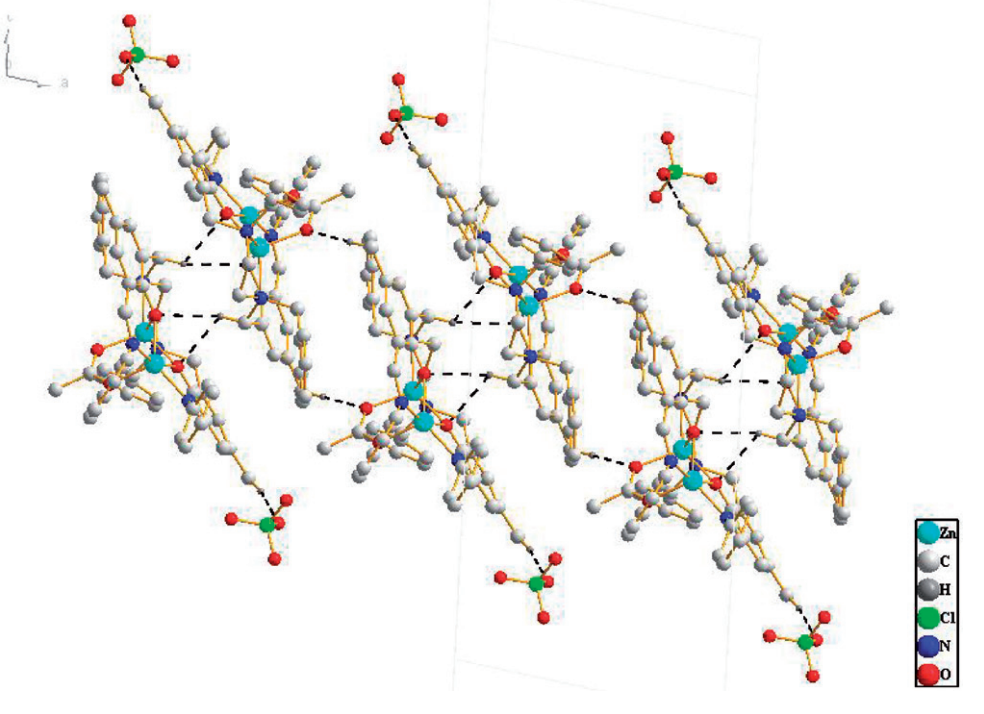


Figure 3. View of the 2-D network depicting the connection *via* C–H···O hydrogen bonds.

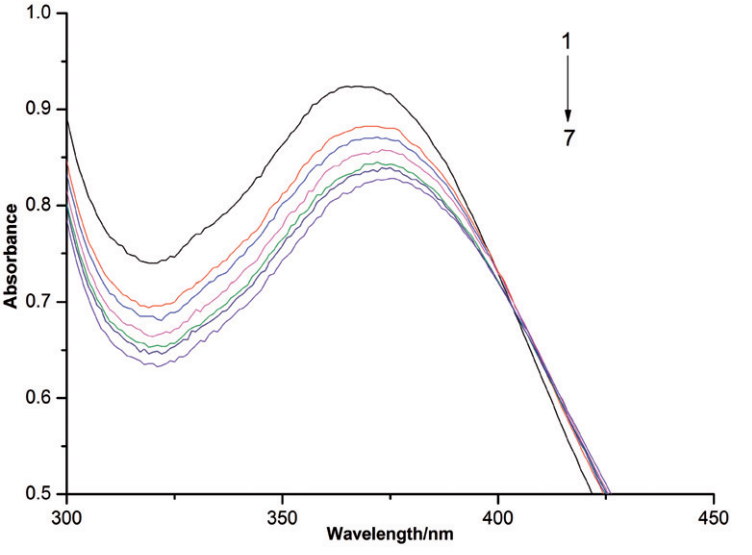


Figure 4. UV-Vis spectra of the Zn(II) complex in the presence of increasing amounts of CT-DNA in 50 mmol $L^{-1}$ Tris-50 mmol $L^{-1}$ NaCl aqueous buffer solution (pH = 7.2). [complex] = 90 μmol $L^{-1}$, [DNA] = 0 (1), 12.8 (2), 16.7 (3), 20.5 (4), 24.2 (5), 27.6 (6), 31.2 (7) μmol $L^{-1}$. The arrow shows the absorbance changing upon increasing DNA concentrations.

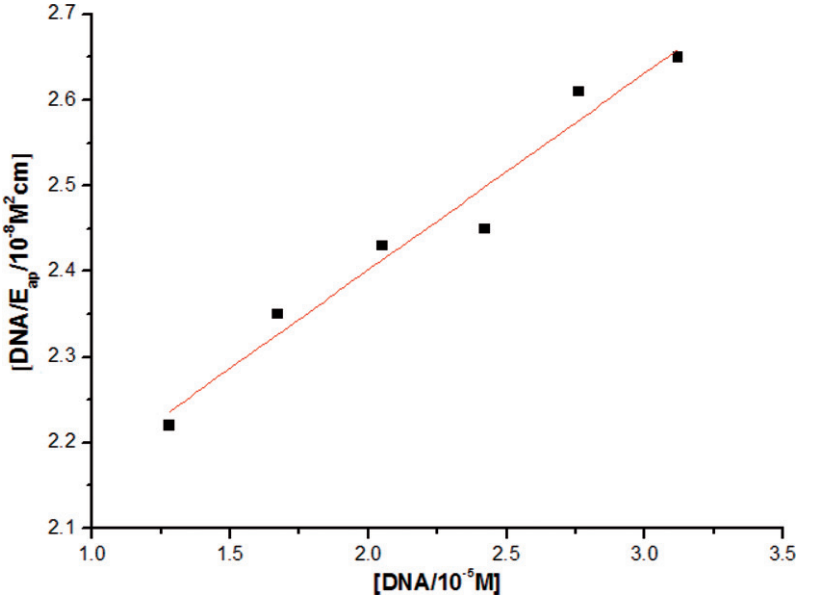


Figure 5. Plot of $[(DNA)/(\varepsilon_a - \varepsilon_f)]$ *vs.* [DNA] for absorption titration of CT-DNA with the complex.

### 3.3. *Kinetic study*

Most dinuclear metal complexes affect phosphate ester hydrolysis, especially phosphomonoester; the distance between two metal ions plays a big role for the hydrolysis rate [33–35]. Macrocyclic dinuclear metal complexes with flexible ligand

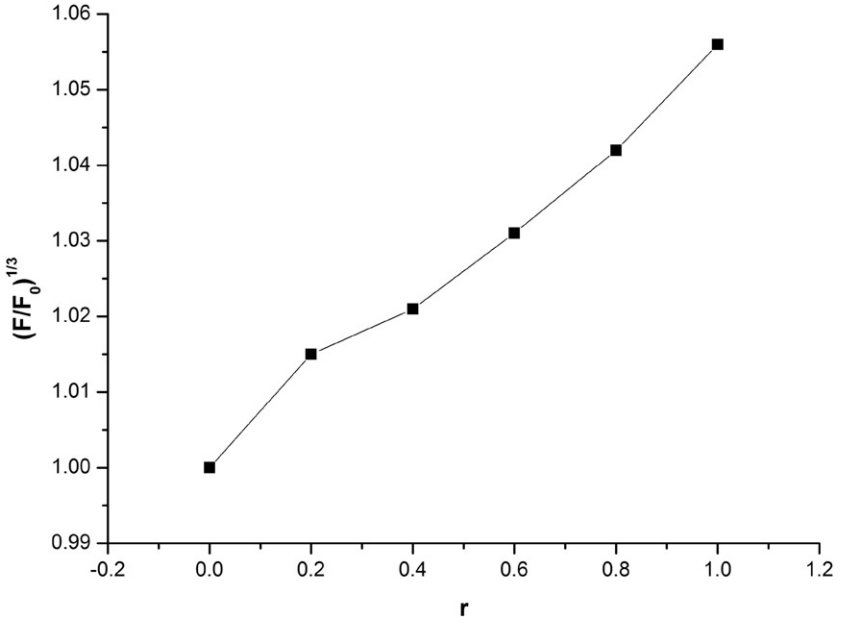


Figure 6. Effects of increasing amounts of the complex on the relative viscosities of CT-DNA at 23.0 (±0.1)°C; [DNA] = 220 μmol $L^{-1}$, $r$ = [complex]/[DNA].

framework tend to give higher hydrolysis because the geometry around metal ions can be regulated during the hydrolysis [18, 19, 36, 37]. There are reports about dinuclear metal complexes catalyzing hydrolysis of phosphate diesters because of unsuitable rigidities and M–M distances [38]. Although noncyclic multinuclear metal complexes show better activity toward phosphate diester hydrolysis, noncyclic flexible structures can decrease the stability of the metal complexes, which are not good candidates for artificial metallonucleases.

The title complex is a macrocycle during the DNA-binding. However, the open-chain ligand provides flexibility toward phosphate ester hydrolysis. The hydrolysis of BNPP promoted by the complex was conducted to mimic phosphate ester hydrolysis activities. Plots of $\ln(A_\infty/A_\infty - A_t)$ *versus* time for BNPP hydrolysis is obtained and shown in figure 7. The pseudo-first-order rate constant $k = 4.23 \times 10^{-5}\,s^{-1}$ was calculated from the slope of the linear plot, indicating an unequivocal hydrolysis activity toward BNPP. This constant is larger than some reported noncyclic dinuclear Zn(II) complexes ($[Zn_2(LH_2)]^{2+}$: $K_b$ is $2.26 \times 10^{-6}\,s^{-1}$ [39]; [$Zn_2L'$]: $K_b$ is $2.5 \times 10^{-6}\,s^{-1}$ [34]; [$Zn_2L$]: $K_b$ ranged from $2.2 \times 10^{-8}\,s^{-1}$ to $3.8 \times 10^{-7}\,s^{-1}$ [33]). In theory, the distance between two Zn(II) ions is 2.971 Å, which should be unsuitable for BNPP hydrolysis [38]. We propose that the good activity toward BNPP hydrolysis can be ascribed to the flexibility of the complex. The constant is also larger than that of mononuclear Zn(II) complexes ([Zn(bpy)$Cl_2$]: $K_b = 5.74 \times 10^{-7}\,s^{-1}$ [40], [Zn(MPGN)]: $K_b = 3.60 \times 10^{-5}\,s^{-1}$ [41]), which can be assigned to the synergetic effect of the metal ions. Overall, we proposed that synergetic effect and the flexibility of the structure of the complex are key factors for hydrolysis activity of the complex.

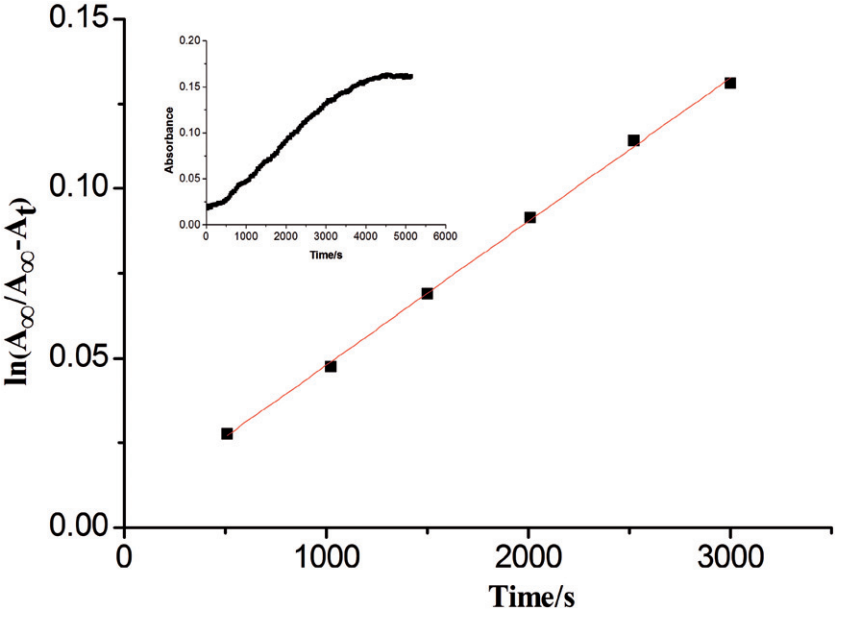


Figure 7. Hydrolysis activity of the complex: plot of $\ln(A_\infty/A_\infty - A_t)$ *vs.* time, inset: plot of absorbance *vs.* time.

## 4. Conclusion

A new macrocyclic dinuclear Zn(II) complex was synthesized by condensation between diamine-bridged dialdehyde and aniline with 1 : 2 molar ratio. The crystal structure shows that the molecule forms a 2-D network by intermolecular C–H$\cdots\pi$ and C–H$\cdots$O hydrogen-bond interactions. Investigation of the interactions of the complex with DNA reveals intercalative binding of the complex with DNA with a binding constant of $1.18 \times 10^4\,\mathrm{mol}^{-1}\,\mathrm{L}$. Moreover, this complex also shows good phosphate hydrolysis activity with formal macrocyclic structure together with flexibility of the complex and synergetic effects as key factors for the high catalytic activity.

## Supplementary material

CCDC-862152 contains the supplementary crystallographic information of this article. These data can be obtained free of charge at www.ccdc.cam.ac.uk/conts/retrieving.html or from the Cambridge Crystallographic Data Centre, 12 Union Road, Cambridge CB2 1EZ, UK [Fax: +44-1223/336-033; Email: deposit@ccdc.cam.ac.uk].

## Acknowledgments

This work was financially supported by the National Natural Science Foundation of China (Nos 20871097, 20971102, 21002076), the Foundation for Midlife and Youth Talent Project of Hubei Province, China (No. Q20111507).

## References


[1] R.F. Hu, J. Zhang, Y. Kang, Y.G. Yao. *Inorg. Chem.*, **8**, 828 (2005).
[2] W. Kobel, M. Hanack. *Inorg. Chem.*, **25**, 103 (1986).
[3] K.S. Min, M.P. Suh. *Solid State Chem.*, **152**, 183 (2000).
[4] H. Oshio, Y. Saito, T. Ito. *Angew. Chem. Int. Ed. Engl.*, **36**, 2673 (1997).
[5] T. Sawaki, Y. Aoyama. *J. Am. Chem. Soc.*, **121**, 4793 (1999).
[6] J.S. Seo, D. Whang, H. Lee, S.I. Jun, J. Oh, Y.J. Jeon, K. Kim. *Nature*, **404**, 982 (2000).
[7] Z.F. Chen, X.Y. Wang, Y.Z. Li, Z.J. Guo. *Inorg. Chem.*, **11**, 1392 (2008).
[8] X. Sheng, X. Guo, X.M. Lu, G.Y. Lu, Y. Shao, F. Liu, Q. Xu. *Bioconjugate Chem.*, **19**, 490 (2008).
[9] P.U. Maheswari, S. Roy, H.D. Dulk, S. Barends, G.V. Wezel, B. Kozlevčar, P. Gamez, J. Reedijk. *J. Am. Chem. Soc.*, **128**, 710 (2008).
[10] Y.F. Chen, L. Wei, J.L. Bai, H. Zhou, Q.M. Huang, J.B. Li, Z.Q. Pan. *J. Coord. Chem.*, **64**, 1153 (2011).
[11] Q.R. Cheng, J.Z. Chen, H. Zhou, Z.Q. Pan. *J. Coord. Chem.*, **64**, 1139 (2011).
[12] J. Pan, L. Cheng, H. Zhou, Z.Q. Pan, Q.M. Huang, X.L. Hu. *Polyhedron*, **29**, 1588 (2010).
[13] Y. He, X.H. Wang, H. Zhou, Z.Q. Pan, J.B. Li, Q.M. Huang. *Inorg. Chem.*, **13**, 314 (2010).
[14] H. Hu, Y.F. Chen, H. Zhou, Z.Q. Pan. *Transition Met. Chem.*, **36**, 395 (2011).
[15] Z.Q. Pan, K. Ding, H. Zhou, Q.R. Cheng, Y.F. Chen, Q.M. Huang. *Polyhedron*, **30**, 2268 (2011).
[16] Q.R. Cheng, Z.Q. Pan, H. Zhou, J.Z. Chen. *Inorg. Chem.*, **14**, 929 (2011).
[17] C. Ding, Y.F. Chen, M. Liu, H.T. Song, H. Zhou, Z.Q. Pan. *Chin. J. Inorg. Chem.*, **28**, 801 (2012).
[18] M. Thirumavalavan, P. Akilan, M. Kandaswamy. *Polyhedron*, **25**, 2623 (2006).
[19] P. Akilan, M. Thirumavalavan, M. Kandaswamy. *Polyhedron*, **22**, 3483 (2003).
[20] SMART and SAINT. *Area Detector Control and Integration Software*, Siemens Analytical X-Ray Systems, Inc., Madison, WI (1996).
[21] G.M. Sheldrick. *SHELXTL V5.1 Software Reference Manual*, AXS Bruker, Inc., Madison, WI (1997).
[22] M.E. Reichmann, S.A. Rice, C.A. Thomas, P. Doty. *J. Am. Chem. Soc.*, **76**, 3047 (1954).
[23] A.M. Pyle, J.P. Rehmann, R. Meshoyrer, C.V. Kumar, N.J. Turro, J.K. Barton. *J. Am. Chem. Soc.*, **111**, 3055 (1989).
[24] G. Cohen, H. Eisenberg. *Biopolymers*, **8**, 45 (1969).
[25] M.E. Reichmann, S.A. Rice, C.A. Thomas, P. Doty. *J. Am. Chem. Soc.*, **76**, 3047 (1954).
[26] A. Neves, M.A. de Brito, I. Vencato, V. Drago, K. Griesar, W. Haase. *Inorg. Chem.*, **35**, 2360 (1996).
[27] B.P. Gaber, V. Miskowski, T.G. Spiro. *J. Am. Chem. Soc.*, **96**, 6868 (1974).
[28] S. Anbu, M. Kandaswamy, P. Suthakaran, V. Murugan, B. Varghese. *Inorg. Biochem.*, **103**, 401 (2009).
[29] J. Qing, W. Gu, H. Liu, F.X. Gao, L. Feng, S.P. Yan, D.Z. Liao, P. Cheng. *Dalton Trans.*, **10**, 1060 (2007).
[30] H. Li, X.Y. Le, D.W. Pang. *J. Inorg. Biochem.*, **99**, 2240 (2005).
[31] J. Sun, S. Shuo, Y. An, J. Liu, F. Gao, L.N. Ji, Z.W. Mao. *Polyhedron*, **27**, 2846 (2008).
[32] V. Lombardo, R. Bonomi, C. Sissi, F. Mancin. *Tetrahedron*, **66**, 2189 (2010).
[33] B. Bauer-Siebenlist, F. Meyer, E. Farkas, D. Vidovic, J.A. Cuesta-Seijo, R. Herbst-Irmer, H. Pritzkow. *Inorg. Chem.*, **43**, 4189 (2004).
[34] J.W. Chen, X.Y. Wang, Y.G. Zhu, J. Lin, X.L. Yang, Y.Z. Li, Y. Lu, Z.J. Guo. *Inorg. Chem.*, **44**, 3422 (2005).
[35] P.E. Jurek, A.M. Jurek, A.E. Martell. *Inorg. Chem.*, **39**, 1016 (2000).
[36] N. Sengottuvelan, D. Saravanakumar, M. Kandaswamy. *Polyhedron*, **26**, 3825 (2007).
[37] S. Aubu, S. Kamalraj, B. Varghese, J. Muthumary, M. Kandaswamy. *Inorg. Chem.*, **51**, 5580 (2012).
[38] J. Du, X.G. Meng, W. Hu, X.C. Zeng. *J. Dispersion Sci. Technol.*, **28**, 199 (2007).
[39] C. Vichard, T.A. Kaden. *Inorg. Chim. Acta*, **337**, 173 (2002).
[40] J. He, J. Sun, Z.W. Maoa, L.N. Ji, H.J. Sun. *Inorg. Biochem.*, **103**, 851 (2009).
[41] R. Bonomi, F. Selvestrel, V. Lombardo, C. Sissi, S. Polizzi, F. Mancin, U. Tonellato, P. Scrimin. *J. Am. Chem. Soc.*, **130**, 15744 (2008).